ISSN 0016-7932, Geomagnetism and Aeronomy, 2019, Vol. 59, No. 8, pp. 1009–1015. © Pleiades Publishing, Ltd., 2019.

The Thin Magnetic Structure of Flare Areas and the Influence of Scale Transformations on the Temperature Profiles of Flares

A. A. Solovyov[a, b, *], E. A. Kirichek[a], O. A. Korolkova[a], L. D. Parfinenko[a], and V. I. Efremov[a]

[a] *Central (Pulkovo) Astronomical Observatory, Russian Academy of Sciences, St. Petersburg, Russia*

[b] *Kalmyk State University, Elista, Republic of Kalmykia, 358000 Russia*

**e-mail: @*

Received February 19, 2019; revised March 18, 2019; accepted April 25, 2019

Abstract—A distinctive feature of chromospheric magnetic fields in the facular regions on the Sun is their very fine spatial structure. In accordance with the observations performed in Ca II K and H line (the level of the lower chromosphere, about 0.5–1 Mm over the photosphere), numerous "slender fibrils mapping the magnetic field" were recorded. It is noted that "...the loops are organized in canopy-like arches" (Jafarzadeh et al., 2017). In this paper we perform some modification of the facular model presented by Solov'ev and Kirichek (2019) as a steady magnetic "fountain" with many thin trickles of plasma flows. The radial-azimuthal temperature profiles of the facula are calculated. It is shown that the difference in the vertical and horizontal scales of the system does not improve the correspondence between the model parameters of the faculae and their observed characteristics.

DOI: 10.1134/S0016793219080206

1. INTRODUCTION

Flare regions on the Sun contain three types of magnetic structures: small-scale force tubes of granular scales; larger and more stable light flare units; and dark micropores and pores—small sunspots without penumbra. The most representative elements of the solar flare fields are flare nodes, which have transverse dimensions of several Mm and a magnetic field from 250 to 1200 Gs. These nodes are generally brighter than those that form in the photosphere and usually have a central dip in the temperature profile, which is an analog of the Wilson depression in sunspots. This dark dip strongly brings the flare nodes very close to the pores and micropores. In general, there is no clear boundary between the indicated classes of structures in the flare area; they can mix or flow into each other. Thus, a flare assembly can be considered a significant thickening of small-scale flare pellets that which most likely occurs at the intersections of the borders of several supergranulation cells. The converging and descending plasma flows at these boundaries, and, most importantly, the markedly lower gas pressure in the intergranular and intersupergranular gaps provide the necessary external conditions to maintain a stable existence of rather large magnetic flare units for a day or more. The central darkening of the flare node is actually a micropore, which dramatically increases its stability. New high-resolution data on the photosphere structure is provided by The Goode Solar Telescope (GST) located at the Big Bear Solar Observatory (California). It has the largest aperture in the world (1.6 m) and can observe the sun in the near-infrared region (Goode et al., 2010). Adaptive optics correct for atmospheric distortion. Small-scale magnetic structures manifest themselves well in the filter patterns in the photospheric spectral line TiO 7057 Å (filter bandwidth 10 Å) and the G band (430.5 ± 0.25 nm) (Sinha, 1991). In this spectral line, bright microstructures appear to be smaller than the achieved resolution (Andic, 2013), and they probably contain magnetic field tubes with a strength of about 1 kG. Figure 1 shows the filtergram of the quiet photosphere obtained on BBSO in the line of TiO 7057 Å (the figure is taken from the official website of BBSO http://www.bbso.njit.edu/~vayur/NST_catalog/2018/05/25/). The dark structure in the center of the image is a micropore with a characteristic diameter of about 0.2 Mm. Micropores are smaller than the photospheric granule and exist for many hours. The area near the micropore contains more extensive adjacent areas of a strong magnetic field, where the granulation pattern is small-scale and irregular (anomalous granulation according to (Dunn and Zirker, 1973)). Figure 1 also shows pores in which there are only hints of darkening in the intensity of the continuum, but they show strong flow concentrations. Narayan and Scharmer (2010) call them protopors or microprotopors. As shown by 1-m images of the Swedish telescope (Lites et al., 2004; Berger et al., 2007), regular annular and semicircular brightenings are observed at high resolution in the vicinity of the

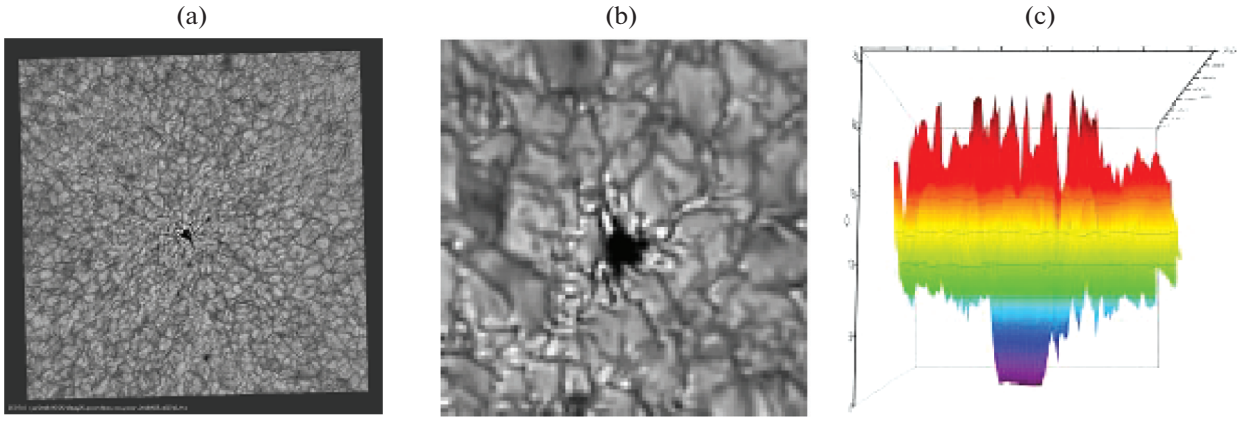

Fig. 1. Left (a): filter photograph of the quiet photosphere obtained with the BBSO telescope on May 25, 2018 at 1622:42 in the TiO 7057 Å line. (taken from http://www.bbso.njit.edu/~vayur/NST_catalog/2018/05/25/). Center (b): a micropore with an annular brightening visible in the central part of the filtration pattern given on an enlarged scale, with a diameter of ~0.2 Mm. Right (c): in color, the photometric surface of this pore, the program "color map surface" is used.

flare assemblies and micropores in white light, which also require interpretation.

An extremely thin fibrous structure of the temperature field is observed in the lower chromosphere in the images in the H and K lines of ionized calcium (Ca II), which form near the temperature minimum level (about 525 km above the photosphere). It reflects the fine structure of the magnetic fields. This is vividly illustrated by Fig. 2 (taken from Jafarzadeh et al., 2017). Such images have been obtained earlier (Pietarila et al., 2009). It should be emphasized that the thin fibers visible on such images do not show any signs of interlacing or mutual overlap, i.e., there is no reason to believe that we are seeing twisted magnetic rope formations.

At the photospheric level, this thin fibrillar structure is obviously obscured by the fairly fast movements of the granulation field, the picture of which completely changes on a scale of 5–10 min. At altitudes of several hundred km, where the photospheric granulation is already "missing," this spatial separation of the magnetic array on quasi-parallel thin fibrils is manifested quite clearly and, most importantly, more stably. The purpose of this work is to build a flare model in a slightly different way than Solov'ev and Kirichek (2019), taking into account the difference between the vertical and horizontal magnetic scales of the system, and to determine how such large-scale transformations change the model parameters of the flare units and whether they help to improve the compliance of the theoretical model with the observed characteristics.

2. MAGNETIC FOUNTAIN WITH THIN JETS

In agreement with the observations, we will assume that the flare magnetic field is represented by a set of nontwisted vertical magnetic force tubes in which the azimuthal field is absent and that the vertical and radial components depend on all three variables r, φ, z in a cylindrical coordinate system:

$$\mathbf{B} = \{B_r(r,\varphi,z)\mathbf{e}_r, 0\cdot\mathbf{e}_\varphi, B_z(r,\varphi,z)\mathbf{e}_z\}. \quad (1)$$

The z axis is directed vertically upwards. Condition $\mathrm{div}\mathbf{B} = 0$ for a field of type (1) has the form

$$\frac{\partial B_z}{\partial z} + \frac{1}{r}\frac{\partial}{\partial r} rB_r = 0. \quad (2)$$

The longitudinal and radial magnetic field can be expressed through the flow function

$$A(r,z) = \int_0^r b_z r dr \quad (3)$$

and some arbitrary dimensionless function of the same flow and angular coordinates $F(A,\varphi)$ in the following way:

$$\begin{aligned} B_z(r,\varphi,z) &\equiv B_0 F(A,\varphi)\, b_z(r,z), \\ b_z(r,z) &= \frac{1}{r}\frac{\partial A(r,z)}{\partial r}, \\ B_r(r,\varphi,z) &\equiv B_0 F(A,\varphi)\, b_r(r,z), \\ b_r(r,z) &= -\frac{1}{r}\frac{\partial A(r,z)}{\partial z}. \end{aligned} \quad (4)$$

Here, $B_0 = \mathrm{const}$ is the unit of measurement of the magnetic field. By substituting (4) into (2), we see that the solenoidality condition (2) is identically satisfied for any choice of the differentiable function $F(A,\varphi)$. The presence of a free function in the distribution of the magnetic field is an extremely important result, not only for the modeling of solar formations but also in a general physical sense. It means that any nontwisted magnetic flux tube can be divided into a number of parallel, arbitrarily thin filaments in which an annular electric current circulates. The dissipation of these numerous, strong (due to the small separation

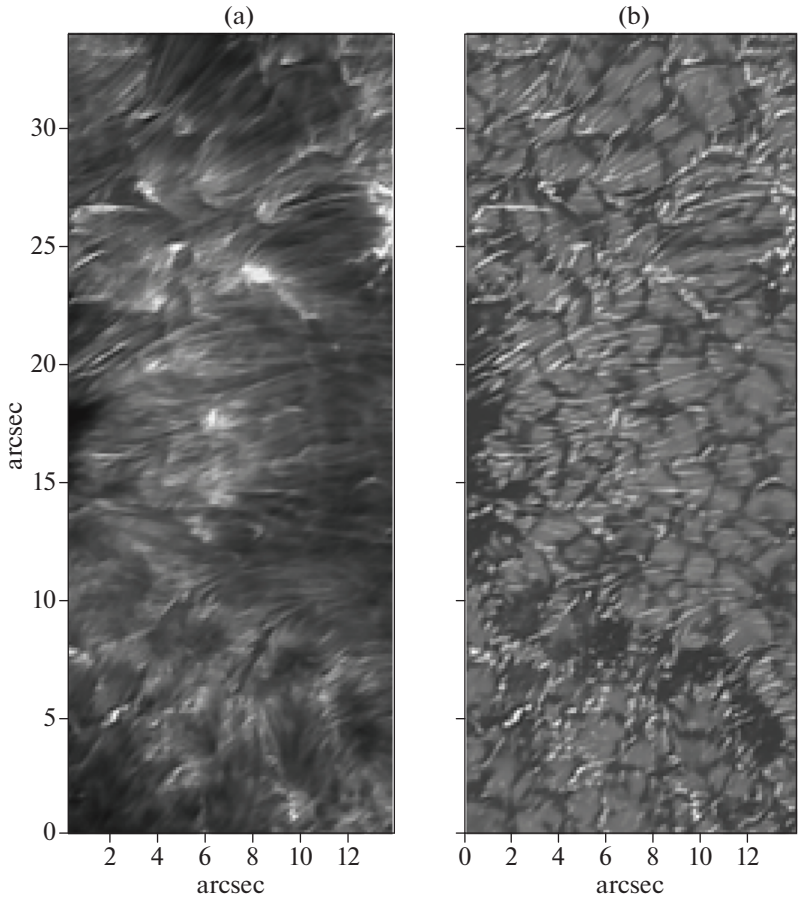

Fig. 2. Taken from Jafarzadeh et al. (2017) (notation: SCF, slender Ca II H fibrils). Panel (a) is Ca II H image. It has been sharpened for better SCF visibility. Panel (b) shows a superposition of SCF identifications on a darkened, low-contrast version of the corresponding 300-nm image.

scale) currents can make, in particular, (along with the dissipation of MHD waves) a noticeable contribution to the direct heating of the plasma due to Joule losses. The dependence of the free function F on the angular coordinates can be selected, e.g., in the following simple form:

$$F^2(A,\varphi) = 1 + f(A,\varphi) = 1 + k^2 \left| A \sum_i a_i \sin(m_i \varphi) \right|, \quad (5)$$

where $f(A,\varphi)$ is the positive oscillating function with the amplitude decreasing with height due to decreasing flow A; a_i, m_i are some positive factors, and k is the inverse length scale. Some interesting effects can be obtained with the selection of different values of the angle parameter m. Thus, at a low value ($m < 1$), we have a strong lateral deformation of the corresponding temperature profile. Large m values describe the fine filamentary structure of the field. If there is no angular dependence of the field, then $F = 1$.

As the basis for a specific description of the magnetic structure of the solar flare, we take the solution Schatzman (1965) in the potential limit:

$$B_z = B_0 J_0(kr)\exp(-kz), \quad B_r = B_0 J_1(kr)\exp(-kz), \quad (6)$$

Here, $J_0(kr), J_1(kr)$ are the Bessel functions of the zero and first orders, B_0 is the magnetic field on the photosphere at $z = 0$. The potential magnetic field does not disturb its environment. In order for the magnetic field to become observable, its shape must differ from the potential and thus cause deviations of the plasma parameters from the background hydrostatics. For this reason, some "force" corrections should be introduced into the field distribution (6). According to Solov'ev and Kirichek (2019), these amendments were (i) the angular dependence of the field as a function F by the formula (5) and (ii) the replacement of the exponent in (6) by the expression

$$Z(z) = 2(\exp(kz) + 1)^{-1}, \quad (7)$$

which describes the blurred Fermi-Dirac step. At $z > 0$, this function tends to $2\exp(-kz)$, i.e., the field approaches the potential. At $z < 0$, the downward magnetic field tends to $2B_0 = \text{const}$. The magnetic field of the flare with this transformation takes the form

$$B_z = B_0 F(A,\varphi) Z(kz) J_0(kr), \quad (8)$$

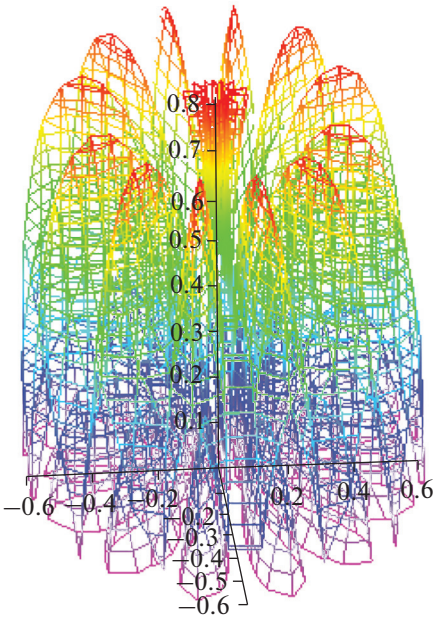

Fig. 3. Example of a 3D magnetic field structure (9) with $\lambda = 1.5$, $k = \frac{1}{0.25\ \text{Mm}}$ $F^2 = 1 + 0.9\exp(-kz)abs(krJ_1(\lambda kr)\sin(25\varphi)$. A magnetic fountain with thin plasma streams along magnetic field lines is very similar to what was observed and numerically simulated by (Jafarzadeh et al, 2017): "... slender fibrils mapping the magnetic field ... loops are organized in canopy-like arches." The units of length in the figure are given in Mm.

$$B_r = B_0 F(A,\varphi)\left[-\frac{\partial Z(kz)}{\partial(kz)}\right]J_1(kr). \tag{9}$$

(We take this opportunity to note that formula (9) in the work by Solov'ev and Kirichek (2019) was typed incorrectly as $B_r = B_0 F(A,\varphi)Z(kz)J_1(kr)$, due to a technical oversight of the authors, although the correct expression was, of course, used in all calculations.)

In this paper, we will somewhat complicate the model: we will take into account that the vertical and horizontal scales of the magnetic configuration may differ from each other. To do this, we introduce a dimensionless positive coefficient λ argument of the Bessel functions and divide the radial component of the field by the same coefficient:

$$B_z = B_0 F(A,\varphi)Z(kz)J_0(\lambda kr), \tag{10}$$

$$B_r = \frac{B_0}{\lambda}F(A,\varphi)\left[-\frac{\partial Z(kz)}{\partial(kz)}\right]J_1(\lambda kr). \tag{11}$$

In this form, the magnetic field satisfies the condition of solenoidality (2). At $\lambda > 1$, the horizontal scale of the flare is smaller than the vertical one; it is as if the flare is pulled upwards. At $\lambda < 1$, the horizontal scale dominates, and the flare is "pressed" to the photosphere. We are interested in how the scale ratio will affect the shape of the temperature profiles of the flare assemblies studied by Solov'ev and Kirichek (2019), assuming $\lambda \equiv 1$. We emphasize here that we retain the stepped structure (7) for the height dependence of the field in the modified version of the model.

The flare knot is immersed in a hydrostatic environment specified by the model of the solar atmosphere of Avrett and Loeser (2008), in which the level with parameters is taken as the basis of the photosphere $T(0) = 6583$ K, $P(0) = 1.228\times10^5$ dyn/cm^2, $\rho(0) = 2.87\times10^{-7}$ g/cm^3, and the layer with the generally accepted photospheric temperature of 5800 K is located 50 km higher.

3. FLARE-TEMPERATURE PROFILES

The analytical methods developed by us (Solov'ev and Kirichek, 2016; 2019) make it possible to calculate the pressure, density, temperature and velocity of plasma flows at each point of the studied magnetic configuration using a given magnetic field structure.

According to our findings (Solov'ev and Kirichek, 2019), the pressure and density of the plasma in the flare tube are set as follows:

$$P(r,z) = P_{ex}(z) + \frac{B_0^2}{8\pi}\left[b_r^2 + 2\int_\infty^r b_z\frac{\partial b_r}{\partial z}dr\right] - \frac{B^2(r,\varphi,z)}{8\pi} + \frac{B_{ex}^2}{8\pi}, \tag{12}$$

$$\rho(r,z) = \rho_{ex}(z) + \frac{B_0^2}{8\pi}\frac{1}{g}\left[2b_r\frac{\partial b_z}{\partial r} - \frac{\partial}{\partial z}\left(b_r^2 - b_z^2 + 2\int_\infty^r b_z\frac{\partial b_r}{\partial z}dr\right)\right]. \tag{13}$$

After substituting here the expressions (10) and (11), as well as the angular dependence (5), we obtain

$$P(r,z,\varphi) = P_{ex}(z) + \frac{B_{ex}^2}{8\pi} - \frac{B_0^2Z^2}{8\pi} \times\left[J_0^2\left(1-\frac{Z''}{\lambda^2Z}\right) + \left(J_0^2 + \left(\frac{Z'}{\lambda Z}\right)^2 J_1^2\right)f(r,\varphi,z)\right], \tag{14}$$

$$\rho(r,z) = \rho_{ex}(z) + \frac{B_0^2k}{8\pi g}2ZZ' \times\left[\left(1-\frac{Z''}{\lambda^2Z}\right)J_1^2 + \left(1-\frac{Z''}{2\lambda^2Z} - \frac{Z'''}{2\lambda^2Z'}\right)J_0^2\right]. \tag{15}$$

The mark over Z indicates differentiation by argument (kz). The plasma temperature in the flare is found from the equation of state of an ideal gas:

$$T(r,\varphi,z) = \frac{P(r,\varphi,z)\mu}{\rho(r,z)\Re}, \tag{14}$$

where $\Re,\mu$ are the gas constant and average molar mass of gas, respectively.

The figures below show the temperature profiles of the flare node at the photospheric level and at the height of the temperature minimum for the same central magnetic field strength at the photospheric level: $B_0 = 1000G$.

3.1. Photospheric Flares, z = 0, T = 6583 K. Central Temperature Dip (place figure 4a, b, c with signatures)

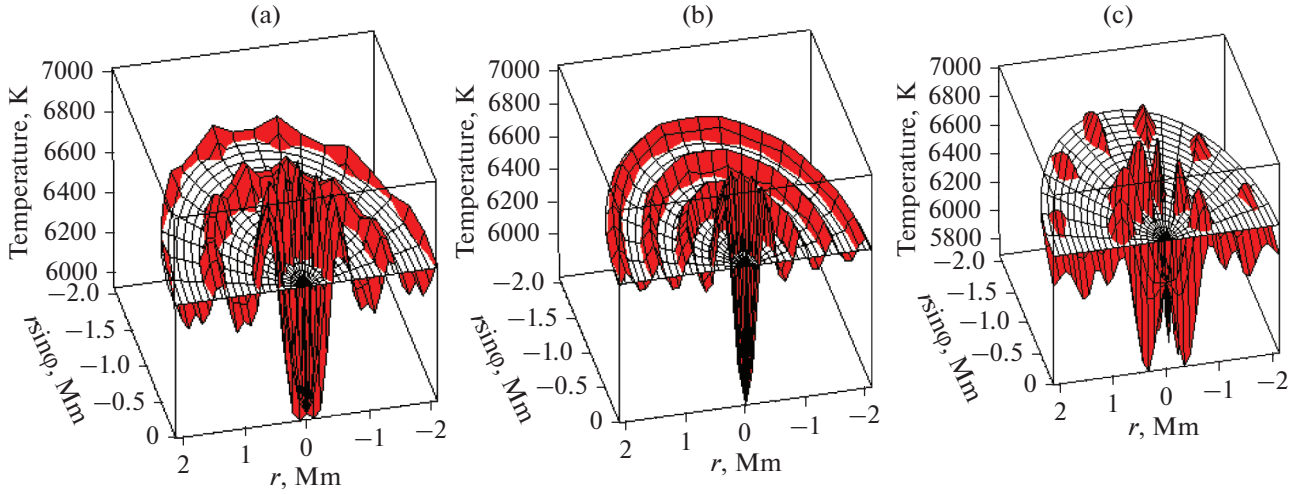

Fig. 4. (a) Temperature profile $T(r, \varphi)$ of the flare node on the photosphere (white plane) at $\lambda = 1$, $a_1 = 3$, $m_1 = 25$, $k = \frac{1}{0.25\ \text{Mm}}$, $B_0 = 1000G$. (b) The same temperature profile but at $\lambda = 1.5$. The central dip has become narrower and deeper, and the azimuthal variations of T are smoothed. (c) The same temperature profile at $\lambda = 0.75$. The central dip is sharply widened and bifurcated, the azimuthal variations of T are enhanced.

3.2. Level of the Temperature Minimum. Chromosphere Temperature of 4410 K (place figure 5a, b, c with signatures)

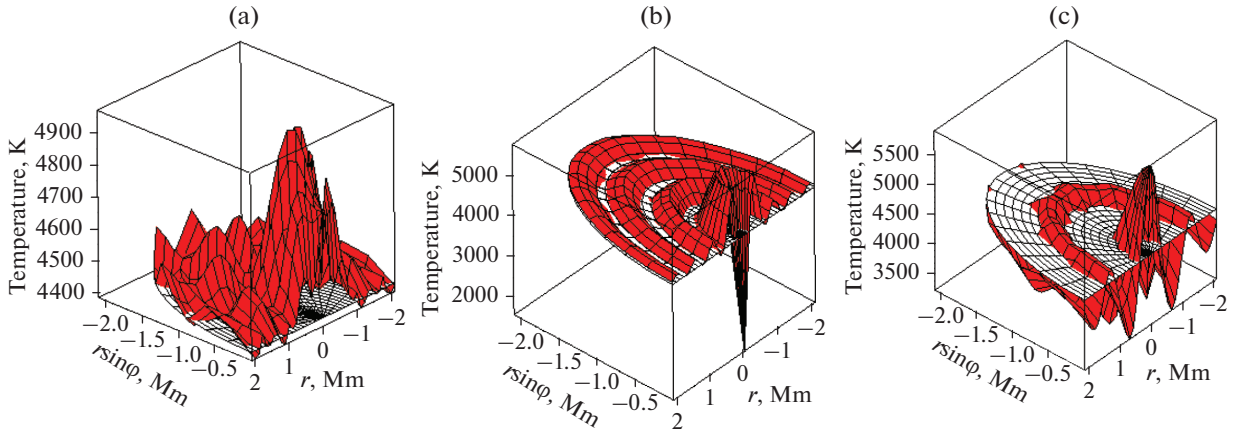

Fig. 5. (a) $\lambda = 1$. T-profile flare when $B_0 = 1000G$, $a_1 = 3$, $m_1 = 25$. The entire profile is above the background (white plane). (b) Same figure at $\lambda = 1.5$. Azimuthal variations are smoothed, and a narrow central dip appeared. (c) $\lambda = 0.75$. Very wide, cold ring around the hot center.

3.3. Radial Fine Structure Modeling (place figure 6a, b, c with captions)

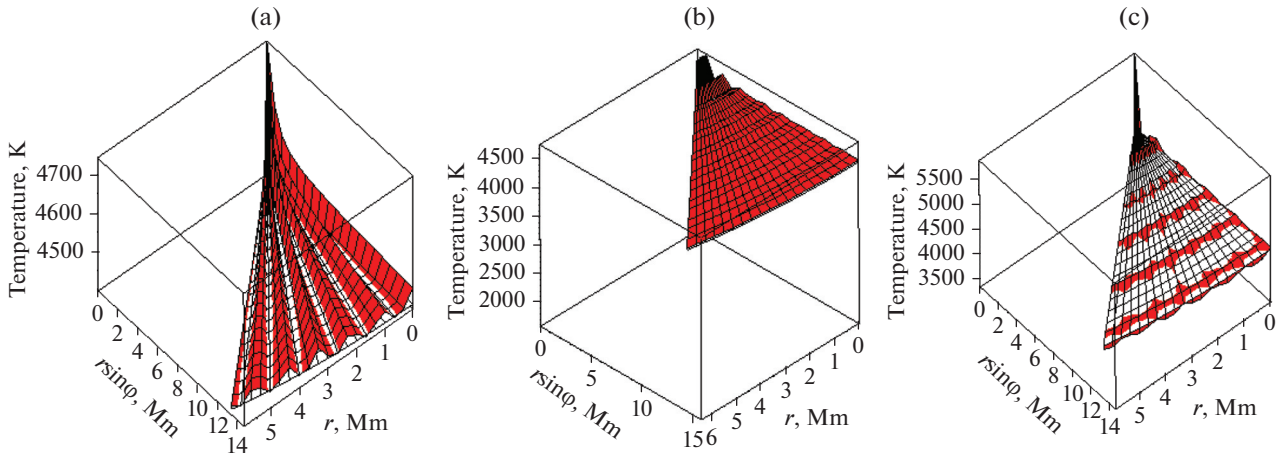

Fig. 6. (a) $\lambda = 1$. The thin extended fibril structure of the flare at the temperature minimum level, which corresponds to the observational data (Fig. 2), is clearly expressed. For clarity, we cut a narrow sector in 24°, $B_0 = 1000G$, $m_1 = 25$, $a_1 = 3$. (b) $\lambda = 1.5$. The same flare as in Fig. 4a. The fibrous radial structure is completely flattened. The central part of the node has a lower temperature. (c) $\lambda = 0.75$. The radial fibrous structure of the fibers is also absent.

4. DISCUSSION

Analysis of Figs. 4a–4c shows that scale transformations do not significantly change the type of flare temperature profiles at the photospheric level. At $\lambda > 1$, the entire flare and its central dip flare becomes narrower; at $\lambda < 1$, the flare is wider, and its central dip splits. It is currently impossible to compare such transformations with observations. However, the profile changes at the level of the temperature minimum at $\lambda \neq 1$ already have a qualitatively different character (Fig. 5 and 6). The most significant thing about altered profiles is that they, at both $\lambda < 1$ and $\lambda > 1$, completely exclude the thin fibrous structure of the chromosphere at this level, which directly contradicts the observations (Fig. 2).

5. CONCLUSIONS

1. The analytical 3D model of a stationary flare unit in the form of a "magnetic fountain" with thin plasma streams along magnetic field lines describes well the main flare features: a fine fibril structure, ring brightening, and characteristic temperature profiles at different heights of the solar atmosphere.

2. The difference between the vertical and horizontal scales does not bring positive moments to the model in terms of a better fit with the observed data. In particular, the thin radial structure of the field at the level of the temperature minimum disappears, which is reliably determined by observations (Jafarzadeh et al., 2017). Apparently, the model of a flare with close spatial scales in the height and horizontal values presented by Solov'ev and Kirichek (2019), is more preferable for the description of the thin filamentary structure of chromospheric layers on the Sun.

FUNDING

This work was supported by grants from the Russian Foundation for Basic Research (project no. 18-02-00168) and the Russian National Science Foundation (no. 15-12-20001).

CONFLICT OF INTEREST

The authors declare that they have no conflicts of interest.

REFERENCES

Andic, A., A small pore observed with a 1.6 m telescope, *Sol. Phys.*, 2013, vol. 282, no. 2, pp. 443–451. https://doi.org/10.1007/s11207-012-0137-z

Berger, T.E., Rouppe van der Voort, L., and Löfdahl, M., Contrast analysis of solar faculae and magnetic bright points, *Astrophys. J.*, 2007, vol. 661, no. 2, pp. 1272–1288.

Dunn, R.B. and Zirker, J.B., The solar filigree, *Sol. Phys.*, 1973, vol. 33, no. 2, pp. 281–304. https://doi.org/10.1007/BF00152419

Goode, P.R., Coulter, R., Gorceix, N., et al., The NST: First results and some lessons for ATS TandEST, *Astron. Nachr.*, 2010, vol. 331, no. 6, p. 620, https://doi.org/10.1002/asna.201011387

Jafarzadeh, S., Rutten, R.J., Solanki, S.K., et al., Slender CAII H fibrils mapping magnetic field in the low solar chromosphere, *Astrophys. J.*, 2017, vol. 229, id 11.

Lites, B.W., Scharmer, G.B., Berger, T., and Title, A.M., Three-dimensional structure of the active region pho-

tosphere as revealed by high angular resolution, *Sol. Phys.*, 2004, vol. 221, pp. 65–84.

Narayan, G. and Scharmer, G.B., Small-scale convection signatures associated with a strong plage solar magnetic field, *Astron. Astrophys.*, 2010, vol. 524, id A3. https://doi.org/10.1051/0004-6361/201014956

Pietarila, A., Hirzberger, J., Zakharov, V., and Solanki, S.K., Bright fibrils in Ca II K, *Astron. Astrophys.*, 2009, vol. 502, pp. 647–660.

Schatzman, E., Model of a force free field. *IAU Symposium*, 1965, vol. 22, pp. 337–345.

Sinha, K. and Tripathi, B.M., Evolution of sunspots seen in molecular lines, Part II, *Bull. Astron. Soc. India*, 1991, vol. 19, pp. 25–36.

Solov'ev, A.A. and Kirichek, E.A., Analytical model of an asymmetric sunspot with a steady plasma flow in its penumbra, *Sol. Phys.*, 2016, vol. 291, no. 6, pp. 1647–1663.

Solov'ev, A.A. and Kirichek, E.A., Structure of solar faculae, *Mon. Not. R. Astron. Soc.*, 2019, vol. 482, no. 4, pp. 5290–5301. https://doi.org/10.1093/mnras/sty3050

SPELL: 1. OK